ACADEMIA ROMÂNĂ
Revue Roumaine de Chimie
http://web.icf.ro/rrch/

Rev. Roum. Chim.,
2018, *63*(11), 1023-1034

EVALUATION OF INTERACTION BETWEEN DNA AND ANTICANCER DRUG TEMOZOLOMIDE AND ITS DEGRADATION PRODUCT BY HPLC

Evin KAPCAK and Hayriye Eda SATANA KARA*

Gazi University, Faculty of Pharmacy, Department of Analytical Chemistry, 06330, Ankara, Turkey

Received November 10, 2017

The aim of this study is an evaluation of the interaction between deoxyribonucleic acid (DNA) and anticancer drug Temozolomide (TMZ) and its degradation product. Such interactions were detected by high-performance liquid chromatography with diode array detector (HPLC-DAD). TMZ is unstable at physiological pH and completely decomposes. Hence, incubations of TMZ and DNA were performed in pH 4.5 acetate buffer. A C18 column and 0.02 M pH 4.5 acetate buffer-acetonitrile (90:10, v/v) as a mobile phase were used. In the chromatograms, it was observed that the peak area values of DNA increased by adding TMZ. This shows that TMZ and DNA are interacting in intercalation mode. Obtained results were verified by absorption and fluorescence spectrometry methods. By using HPLC and spectrophotometric methods, binding constants were calculated as 3.7×10^4 M^{-1} and 2.6×10^4 M^{-1}, respectively. Besides, the interaction of degradation product of TMZ and DNA was also investigated.

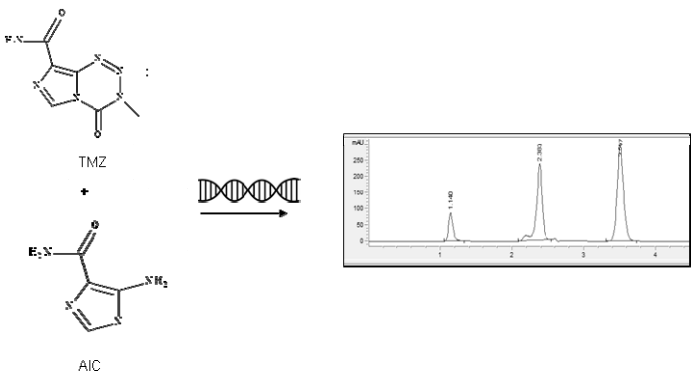

INTRODUCTION

Temozolomide (TMZ), 3-methyl-4-oxo-3,4-dihydroimidazo[5,1-d][1,2,3,5]tetrazin-8 carboxamide, is a kind of an alkylating agent. This anticancer drug is used for the treatment of melanoma, leukemia, and brain cancer such as glioblastoma multiforme by the oral way. [1,2] TMZ shows antitumor effect through its alkylating/ methylating ability to DNA, which most often occurs at the N7 or O6 position of guanine. This reaction inhibits the DNA, RNA, and protein synthesis, damages to DNA, and deaths of tumor cells. TMZ is a prodrug and an imidazotetrazine derivative of the dacarbazine, (5E)-5-(dimethyl-aminohydrazinylidene) imidazole-4-carboxamide, (DTIC). TMZ demonstrates better antitumor activity and safer in clinical applications.[3,4] Antitumor activity of drug depends on linear triazine group, (5E)-5-(methylaminohydrazinylidene) imidazole-4-carboxamide (MTIC). DTIC is metabolically converted to MTIC in the liver, whereas TMZ is degraded chemically to MTIC at physiological pH. [5] The MTIC causes alkylation of guanine at the O6 and N7 positions, thus it shows cytotoxic effect. After this process, MTIC converts itself to 5(4)- aminoimidazole-4(5)-carboxamide (AIC) (Fig. 1).[6,7] AIC is an intermediate molecule responsible for the synthesis of purines. This reduction reaction is irreversible and is pH-dependent. At room temperature and physiological pH, AIC is stable while the MTIC is not stable. However, TMZ is stable in the pH <5 and does not show any degradation reaction.

* Corresponding authors: eda@gazi.edu.tr

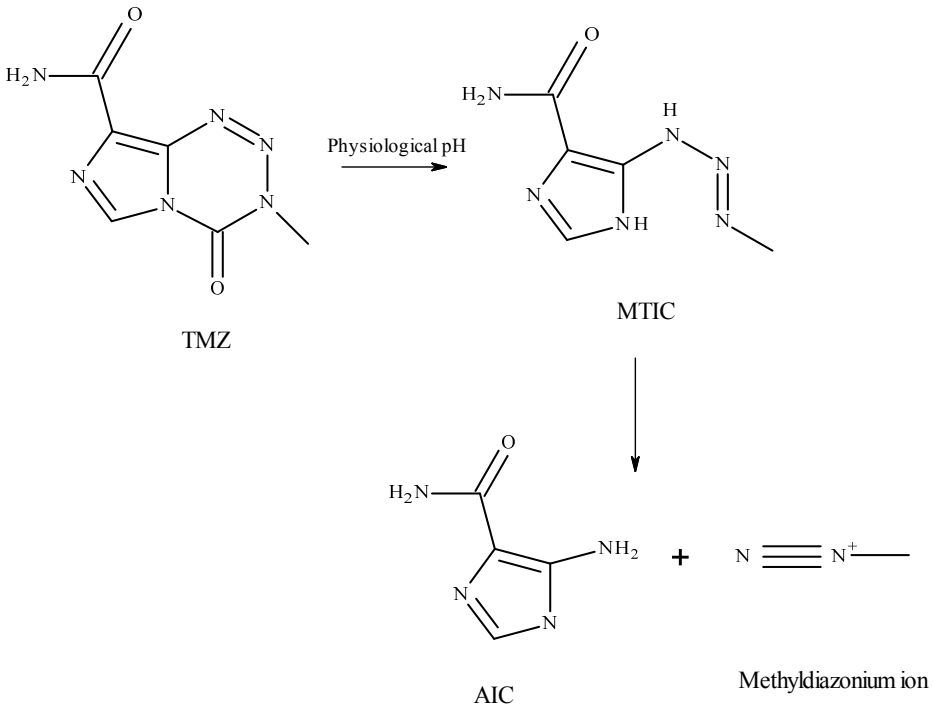

Fig. 1 – Hydrolysis cascade of TMZ.

Considering that as a prodrug TMZ and its degradation products are pharmacologically active, a few methods have been described for the analysis of TMZ and its metabolites in aqueous media, such as HPLC with UV[8-13] or MS/MS detector,[14] micellar electrokinetic capillary electrophoresis (MEKC),[15] spectrophotometry,[16] and voltammetry.[17,18]

DNA has an important biological role in the life process as a genetic material. DNA is often the target molecule for ions, carcinogens, and drugs. Especially anti-cancer drugs interact with DNA to show their activities. This interaction often results strand breaks, chromosome abbreviations, mutations and finally degradation of DNA replication and division. These events lead to increasing of carcinogenic or teratogenic risks and cell death. Therefore, the investigation of DNA-drug interaction is needed to design DNA-targeted drugs and understand the mechanism of drug action. For these reasons, several methods have been developed for the analysis of DNA-drug interaction. In these methods, especially electrochemical and spectroscopic methods such as UV-vis, luminescence, circular dichroism, Raman, and NMR[19-25] are widely used separately or generally together to verify the obtained results. Additionally, separation techniques such as chromatography[26-28] and capillary electrophoresis[29] rarely have been performed in order to make the investigation of interaction. In HPLC methods, the incubated species are separated on the column and the free and/or bound ligands are monitored from the corresponding peaks. The method is only applicable if there is no dissociation during the resolution through the separation column. This limitation causes less application to the method.

In the literature survey, there are few methods about the interaction of TMZ-DNA. These methods based on electrochemical[30- 32] and spectroscopic[33] techniques. However, the interaction of DNA and TMZ/ chemical degradation product by HPLC has not been carried out.

The aim of this work was to investigate the characterization of the binding affinity of TMZ to DNA via direct separation method. The preincubated mixture containing the drug and the DNA is injected into a reverse phase chromatographic column. The data obtained by HPLC were supported by spectroscopic studies. For this purpose, the binding properties of TMZ with DNA were also studied by UV-Vis absorption spectroscopy and fluorescence emission spectroscopy which provided important proofs for detailed understanding the anticancer property of TMZ. In addition to this, TMZ is unstable in a solution and quickly decomposes to a degradation product which interacts with the DNA. In the present study interaction of degradation product and DNA was also identified.

RESULTS AND DISCUSSION

pH effect studies

For identification of pH effect on TMZ and DNA signals, acetate buffer (pH3.5-5.5), phosphate buffer (pH 6.0-8.0), borate buffer (pH 9.0), 0.1 M HCl, and 0.1 M NaOH solutions were examined. According to the absorption spectra, the highest absorbance value for TMZ was obtained by using pH 4.5 acetate buffer. Besides, it is reported in the literature that TMZ is stable in the medium pH<5. In addition, DNA is also stable at this pH. Therefore, pH 4.5 acetate buffer was selected as a mobile phase.

Optimization and Validation of Chromatographic Conditions

In the beginning of the study, the optimization studies were performed to optimize the separation conditions. For this purpose, column, mobile phase composition, pH, flow rate, and column temperature were tested. In order to evaluate the effect of the column, C8 and C18 columns were tested and well-shaped and symmetrical peaks with good separation were obtained with C18 column. Methanol and acetonitrile were tried as an organic phase. With the using of methanol, the peak of TMZ had a shoulder and tailing factor of the peak was more than 2. Therefore, acetonitrile was selected as an organic solvent. For optimization of organic phase ratio, 10%, 20%, and 30% values were performed. When the organic phase ratio was above 10%, peak tailing was observed and the retention time was rather short for the good separation. According to these results, acetate buffer (0.02 M, pH 4.5)–acetonitrile (90:10, v/v) was found most suitable as a mobile phase for TMZ-DNA interaction analysis using DAD detection at 260 nm. To identify the temperature effect on the separation, temperatures between 15 ºC and 40 ºC were examined. It has been observed that the temperature affects both the separation and the peak symmetries; hence, 30 ºC was selected as an optimized temperature. The flow rate almost never affected the resolution but changed the retention time. Different flow rates, 0.8 mL/min, 1 mL/min, and 1.3 mL/min, were examined and optimum results were obtained at 0.8 mL/min. Under these optimized conditions retention times of DNA, degradation product and TMZ were 1.1, 2.3 and 3.5 min, respectively. The proposed method was successfully used for the estimation of the interaction of TMZ and its degradation product with DNA.

After the optimization studies, validation parameters were realized. Therefore, system suitability test for the proposed method was performed. For this purpose, such parameters as theoretical plate number, capacity factor, tailing factor, resolution, symmetry factor, retention time, and RSD % of peak area for ten repetitive injections were calculated for both TMZ and DNA. The obtained results of system suitability tests were found within acceptable limits and in agreement with the USP requirements (Table 1).

System repeatability was determined by six replicate applications at three different concentrations of TMZ (5.2×10^{-5}, 2.6×10^{-4}, and 5.2×10^{-4} M) and DNA (2.03×10^{-6}, 1.02×10^{-5}, and 2.03×10^{-5} M) on the same day (intra-day precision). Inter-day precision was specified by the assay of similar concentrations of analytes and followed for three different days. The obtained results were summarized in Table 2 which indicated a high degree of precision of the proposed method.

A robustness test was conducted to determine whether the developed method was affected by minor changes in the analysis parameters. Hence, organic phase ratio (8-10-12 %), pH value (4.3-4.5-4.7), temperature (27-30-33), flow rate (0.7-0.8-0.9), and wavelength parameters (258-260-262) were evaluated. The robustness tests were carried out at 2.6×10^{-4} M of TMZ and 1.02×10^{-5} M of DNA. For all parameters, RSD% values were smaller than 2% which indicated that minor changes in the system did not lead to significant differences in peak areas.

Interaction Studies

Chromatographic Analysis

In order to identify the interaction of drug-DNA, HPLC method was used. For this purpose, at the first stage, DNA and TMZ solutions prepared at five different concentrations were separately injected into the HPLC system and chromatograms were obtained. Secondly, two different solution groups were prepared as mentioned before for chromatographic determination of drug-DNA interaction and peak area values were recorded. In the first solution group; TMZ solution was added at increasing concentrations to the 1.02×10^{-5} M DNA solution while in the second group a DNA solution was added to the 2.6×10^{-4} M TMZ solution at increasing concentrations. The solutions in each group were prepared in three parallel. The obtained chromatograms show three peaks related to DNA, degradation product of TMZ, and TMZ

with the retention times 1.1, 2.3 and 3.4 minutes, respectively. Chromatograms at the end of 1st, 2nd, 3th and 6th hours of incubation times were recorded to investigate for the time optimization studies of these two solution groups. The chromatograms of the first group show that peak area values of DNA increase with the increasing time. In the second group, the peak values of TMZ decreased while unknown peak increased with the time (Tables 3 and 4). The sixth-hour-incubation time was selected for the analysis and data from these experiments were shown briefly in Table 5 and the chromatogram was given in Fig. 2.

Table 1

System suitability parameters

Parameters	Calculated Values	
	TMZ	DNA
Theoretical Plate Number (N)	7964	3704
Capacity Factor (k′)	1.39	1.16
Tailing Factor (T)	1.05	1.02
Resolution (R_S)	5.05	8.01
Symmetry Factor	0.99	1.01
RSD% of peak area	0.08	0.06
Retention time (t_r)	3.5	1.1

Table 2

The results of intra- and inter-day precision

	DNA	(RSD %)*	TMZ	(RSD %)*
Inter-day precision (M)	$2.03x10^{-6}$	1.01	$5.2x10^{-5}$	0.12
	$1.02x10^{-5}$	0.84	$2.6x10^{-4}$	0.03
	$2.03x10^{-5}$	0.39	$5.2x10^{-4}$	0.04
Intra-day precision (M)	$2.03x10^{-6}$	0.92	$5.2x10^{-5}$	0.08
	$1.02x10^{-5}$	0.78	$2.6x10^{-4}$	0.11
	$2.03x10^{-5}$	0.34	$5.2x10^{-4}$	0.08

* Each value is the mean of six experiments

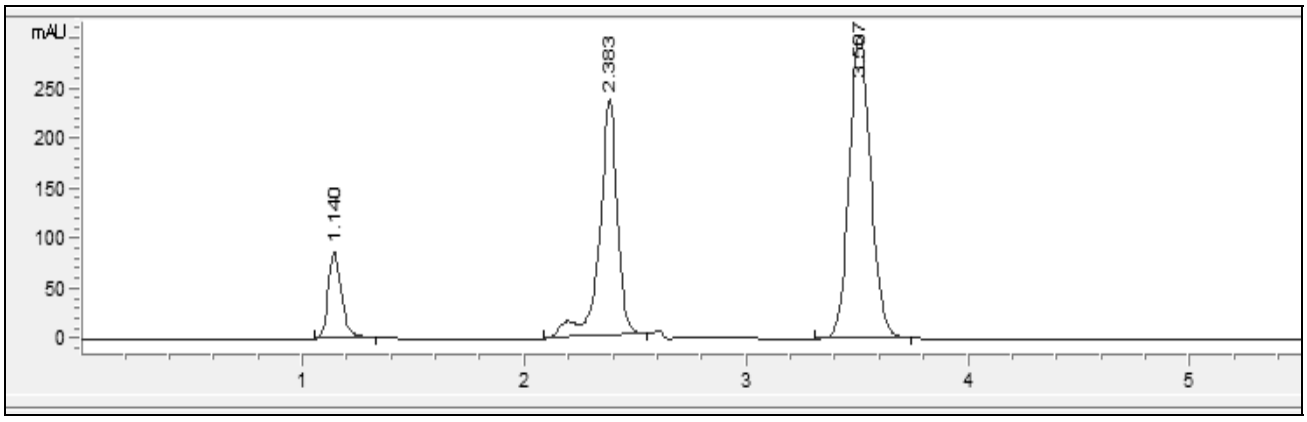

Fig. 2 – The chromatogram of 1.02×10^{-5} M DNA and 2.6×10^{-4} M TMZ solution after six hour-incubation time.

Table 3

Peak area values of 1.02×10^{-5} M DNA and TMZ at increasing concentration

	1.02×10^{-5} M DNA Area	TMZ (M)	Unknown Area	TMZ Area
Before interaction	141.6	5.2×10^{-5}	52.7	561.2
		1.3×10^{-4}	92.1	1414.3
		2.6×10^{-4}	269.4	2726.2
		3.9×10^{-4}	432.5	4131.8
		5.2×10^{-4}	873.6	5599.3

Tabel 3 (continued)

First hour	142.8	5.2×10^{-5}	68.3	533.14
	144.0	1.3×10^{-4}	118.4	1325.8
	164.2	2.6×10^{-4}	274.7	2701.8
	182.2	3.9×10^{-4}	414.6	3992.2
	197.0	5.2×10^{-4}	839.0	5437.6
Second hour	145.4	5.2×10^{-5}	76.5	504.8
	152.0	1.3×10^{-4}	130.9	1290.8
	174.9	2.6×10^{-4}	307.2	2636.9
	191.3	3.9×10^{-4}	430.8	3896.0
	208.2	5.2×10^{-4}	894.6	5324.4
Third hour	175.0	5.2×10^{-5}	87.9	496.3
	193.4	1.3×10^{-4}	138.0	1217.8
	217.6	2.6×10^{-4}	292.3	2450.3
	275.9	3.9×10^{-4}	464.9	3590.5
	331.4	5.2×10^{-4}	656.1	4957.6
Sixth hour	297.6	5.2×10^{-5}	209.4	484.7
	330.8	1.3×10^{-4}	543.7	1176.1
	374.9	2.6×10^{-4}	1319.1	2053.8
	446.9	3.9×10^{-4}	1673.4	2735.4
	535.5	5.2×10^{-4}	2275.1	3272.4

Table 4

Peak area values of 2.6×10^{-4} M TMZ and DNA at increasing concentration

	2.6×10^{-4} M TMZ Area	DNA (M)	Unknown Area	DNA Area
Before interaction	2726.2	2.03×10^{-6}	52.7	30.4
		5.08×10^{-6}	92.1	66.8
		1.02×10^{-5}	269.4	141.6
		1.52×10^{-5}	432.5	217.8
		2.03×10^{-5}	873.6	267.4
First hour	2653.9	2.03×10^{-6}	156.2	40.2
	2710.9	5.08×10^{-6}	281.3	86.7
	2701.8	1.02×10^{-5}	274.7	164.2
	2627.3	1.52×10^{-5}	295.9	343.3
	2527.8	2.03×10^{-5}	983.5	456.9
Second hour	2486.0	2.03×10^{-6}	183.9	45.3
	2654.0	5.08×10^{-6}	271.5	96.3
	2636.9	1.02×10^{-5}	307.2	174.9
	2540.0	1.52×10^{-5}	307.8	389.6
	2443.5	2.03×10^{-5}	1167.0	534.0
Third hour	2413.7	2.03×10^{-6}	197.6	58.8
	2488.1	5.08×10^{-6}	280.3	124.7
	2450.3	1.02×10^{-5}	292.3	217.6
	2357.3	1.52×10^{-5}	339.3	459.0
	2267.1	2.03×10^{-5}	1668.9	636.0
Sixth hour	2322.0	2.03×10^{-6}	216.1	117.0
	2185.3	5.08×10^{-6}	418.3	259.9
	2053.8	1.02×10^{-5}	1332.6	374.9
	1921.4	1.52×10^{-5}	1634.7	539.8
	1844.1	2.03×10^{-5}	2114.6	749.9

Table 5

Peak area changes obtained 6-hour-incubation time

1.02×10^{-5} M DNA Area	TMZ (M)	DNA Area	Unknown Area	TMZ Area
	5.2×10^{-5}	297.6	209.4	484.7
	1.3×10^{-4}	330.8	543.7	1176.1
141.6	2.6×10^{-4}	374.9	1319.1	2053.8
	3.9×10^{-4}	446.9	1673.4	2735.4
	5.2×10^{-4}	535.5	2275.1	3272.4
2.6×10^{-4} M TMZ Area	DNA (M)			
	2.03×10^{-6}	117.0	216.1	2322.0
	5.08×10^{-6}	259.9	418.3	2185.3
2726.2	1.02×10^{-5}	374.9	1332.6	2053.8
	1.52×10^{-5}	539.8	1634.7	1921.4
	2.03×10^{-5}	749.9	2114.6	1844.1

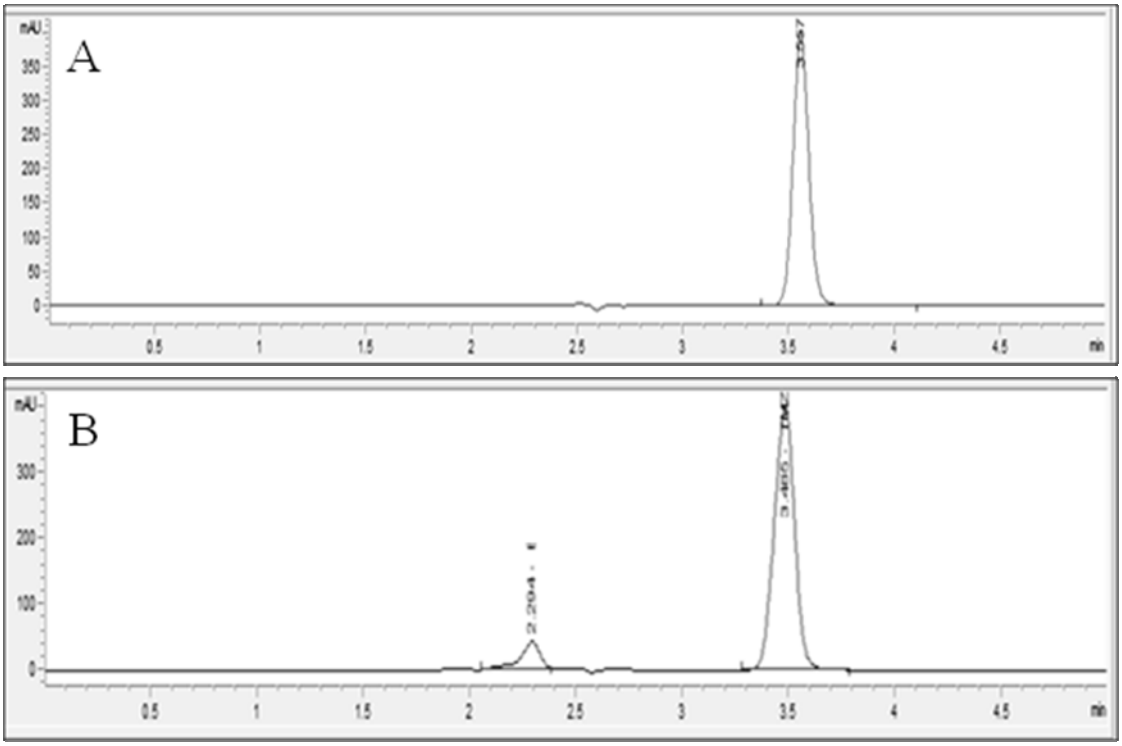

Fig. 3 – Chromatograms of 2.6×10^{-4} M TMZ standard solutions prepared in (A) pH 4.5 acetate buffer and (B) deionized water.

Table 6

Peak areas changes of unknown and TMZ for HPLC

	Deionized water		pH 4.5 acetate buffer	
Time (min)	Unknown Peak Area	TMZ peak area	Unknown Peak Area	TMZ peak area
0	99.1	1084.6	19.9	1126.3
30	110.6	1080.3	20.8	1123.5
60	133.1	1076.0	20.5	1125.7
120	463.7	905.0	20.1	1124.1
180	1133.8	729.4	20.2	1126.8
240	1314.4	358.5	20.6	1124.2
300	1695.0	314.8	20.4	1124.9
360	1699.0	311.2	20.4	1121.7

In order to identify an unknown peak, the new experiments were designed. Previous studies show that TMZ chemically degrades to MTIC and then finally to AIC both *in-vivo* and *in-vitro* conditions at physiological pH (pH 6-7).[13,16] For degradation of TMZ, preparation and all dilutions were made with deionized water. The pH value of aqueous solution was at about 8.5 which causes the degradation of TMZ. As a result of this experiment, a new peak appeared at 2.3 min compatible with previous results and belongs to an unknown species (Fig. 3). A 6-hour-stability test was performed for chromatographic studies. When chromatograms were examined, it was observed that the peak area of TMZ decreased with time while the peak of the unknown species increased without changes in the retention times (2.3 for unknown and 3.5 min for TMZ) of both species. Whereas, the values of the TMZ and the unknown species prepared in the buffer solution show any change (Table 6). In order to better understand, similar experiments were repeated by absorption spectrophotometry. A time-dependent decrease in peak intensity was observed in the spectrum of the TMZ solution prepared with deionized water. Compared with the spectra of the TMZ and AIC species obtained from the literature[16] and the three-dimensional spectrum obtained from the DAD detector, it is suggested that the unknown species belongs to AIC. AIC, the degradation product of TMZ, also interacts with DNA. When the drug concentration was kept constant and the DNA concentration increased, the peak areas of the AIC are increased while the peak areas of the TMZ decreased. It can be said that the decrease in the peak area of the drug and the increase of the peak area of AIC may have resulted from interaction with DNA not degradation.

The interaction of TMZ and AIC with DNA were simultaneously identified. Based on the variations in the peak area values of TMZ upon binding to ds-DNA, the binding constant (*K*) was calculated according to Benesi-Hildebrand equation.[36] The plot of $A_0/(A-A_0)$ *vs* 1/[DNA] was constructed using the data from the chromatograms. In here A_0 and A were peak area values of TMZ in the absence and presence of DNA. The binding constant (*K*) was calculated from the plot and found $3.7\times 10^4\ M^{-1}$ for TMZ-DNA which suggests moderate intercalative binding. For the calculation of binding constant of AIC-DNA, a similar approach was used and calculated as $5.04 \times 10^4\ M^{-1}$.

UV-vis Absorption Spectral Analysis

UV-vis absorption spectroscopy has a widespread use in determining the stability of DNA and its interaction with small molecules. The UV-vis spectrum of DNA shows a broad band spectrum between 200-350 nm and has the maximum absorption at 260 nm due to chromophore groups at purine and pyrimidine bases. TMZ also has a broad absorption band in the range 200-420 nm with three maxima at 224, 256 and 330 nm.

In order to investigate the interaction mechanism of TMZ and DNA, spectrophotometric titration technique has been carried out. A considerable decrease in absorption was observed when adding DNA to the solution of the TMZ (Fig. 4). In addition to this study, the TMZ solution in the same concentration was titrated with only the buffer solution to study the effect of the dilution. From the obtained spectra, it is seen that the decrease of the peak values of TMZ is due to the interaction with DNA, not dilution. This hypochromic effect on the spectra of the DNA-TMZ mixture suggested that a binding event may have occurred by intercalation.

The binding constant (*K*) was calculated according to the Benesi-Hildebrand equation (Eq 1).

$$A_0/(A - A_0) = \varepsilon_T/(\varepsilon_C-\varepsilon_T) + \varepsilon_T/(\varepsilon_C-\varepsilon_T) \times 1/K\,[\mathrm{DNA}] \quad (1)$$

where A_0 and A are the absorbance values of TMZ in the absence and presence of ds-DNA, ε_T and ε_C are the absorption coefficients of TMZ and its complex with ds-DNA, respectively. The plot of $A_0/(A-A_0)$ *vs* 1/[DNA] was constructed using the data from the absorbance titrations and a linear fitting of the data yielded the binding constant $K= 2.6 \times 10^4\ M^{-1}$ for TMZ-DNA (Fig. 4 inset).

Absorption spectroscopy is commonly used to determine the binding characteristics of molecules with DNA. The well-known interaction modes of molecules and DNA are electrostatic, groove binding, and intercalative interactions. Generally, the interaction of small molecule and DNA causes to form a complex molecule, change in absorbance (hypochromic or hyperchromic effect) and shift in wavelength (red or blue shift). If this binding is a stronger mode such as intercalation, the intensity of absorption will decrease and maximum wavelength shifts to longer way due to π-π stacking from the aromatic planar structure and the base pairs of DNA. But, if the interaction mode is electrostatic or groove binding, shifting effect does not appear. Considering the planar character of TMZ, intercalative binding mode of TMZ with DNA should be proposed. However, in this study, the hypochromic effect was observed while no shifting effect existed. This phenomenon may be attributed to moderate intercalation of TMZ and DNA.

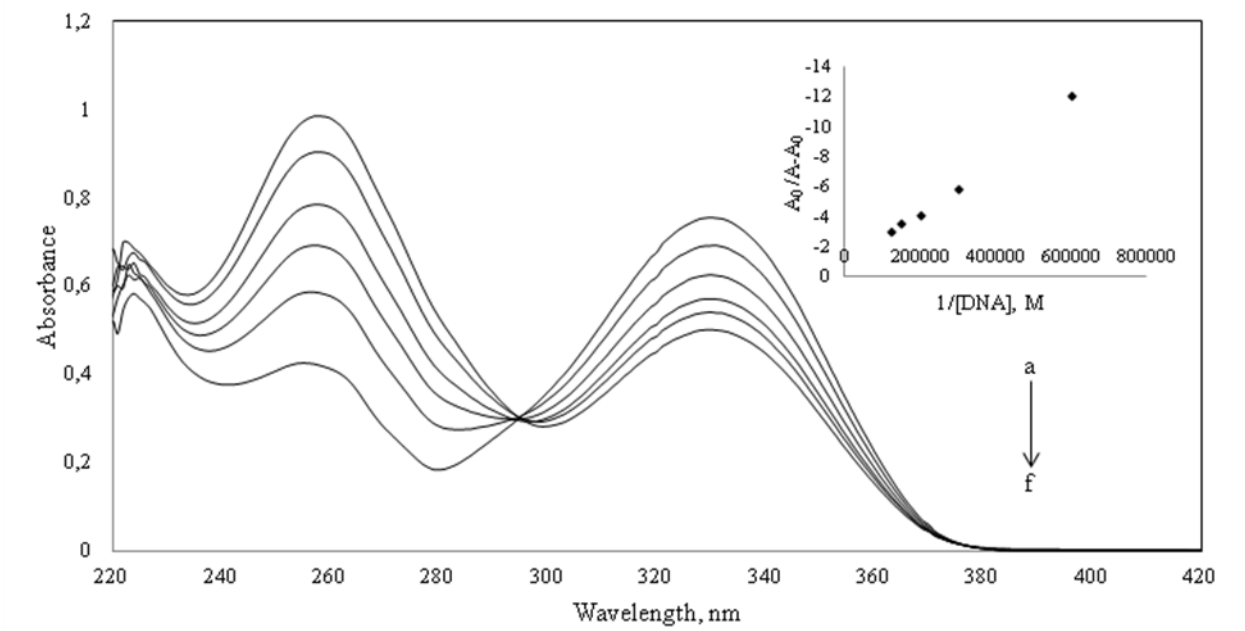

Fig. 4 – Absorption spectra of TMZ in the presence of different concentrations of DNA C_{TMZ}= 8.32 ×10^{-5} M (a) and C_{DNA}= 1.66×10^{-6} M (b), 3.32×10^{-6} M (c), 4.98×10^{-6} M (d), 6.64×10^{-6} M (e) and 8.3×10^{-6} M (f). The inset shows the plot of $A_0/(A-A_0)$ *versus* 1/[DNA] for TMZ-DNA.

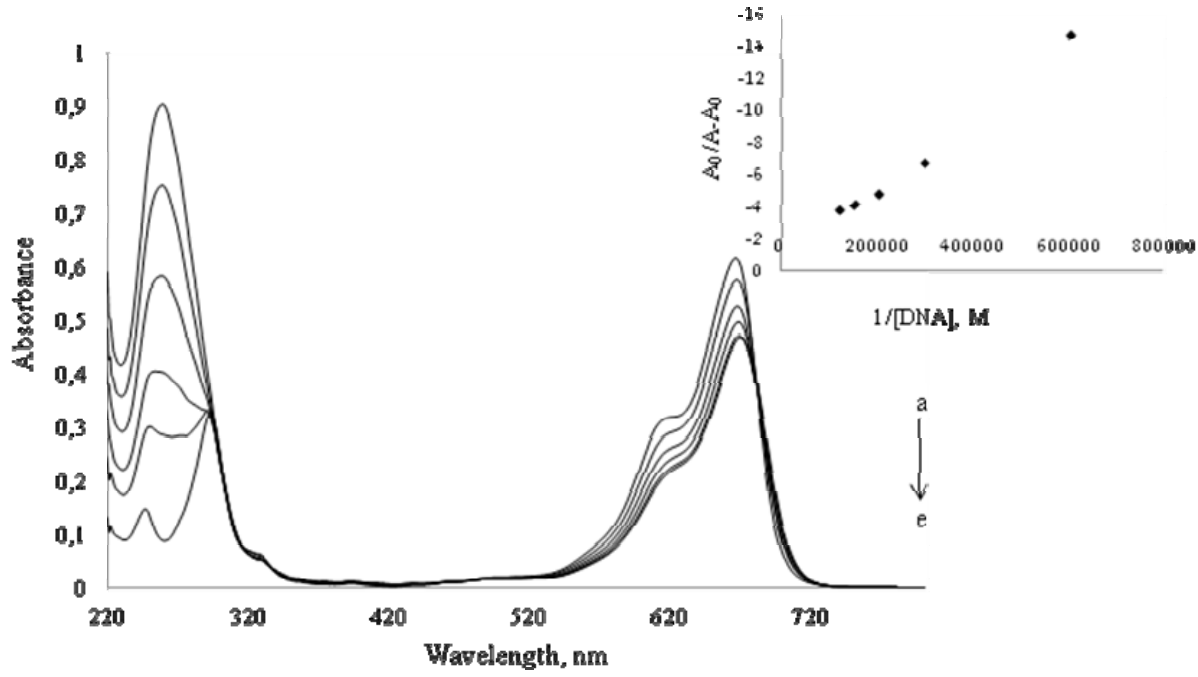

Fig. 5 – Absorption spectra of MB in the presence of different concentrations of DNA. C_{MB}= 1.0 ×10^{-5} M (a) and C_{DNA}= 1.66×10^{-6} M (b), 3.32×10^{-6} M (c), 4.98×10^{-6} M (d), 6.64×10^{-6} M (e), and 8.3×10^{-6} M (f). The inset shows the plot of $A_0/(A-A_0)$ *versus* 1/[DNA] for MB-DNA.

Competitive Binding Studies by Fluorescence Spectroscopy

The competitive method was used to determine DNA-TMZ interaction because both DNA and TMZ did not show fluorescence properties. For this purpose, MB was used as an intercalative probe. MB is a planar aromatic ring which belongs to phenothiazine class and has a cationic charge. MB binds specifically guanine bases in DNA and interacts with intercalation mode. MB is a highly fluorescent molecule, but its fluorescence intensity quenched when interacting with DNA.

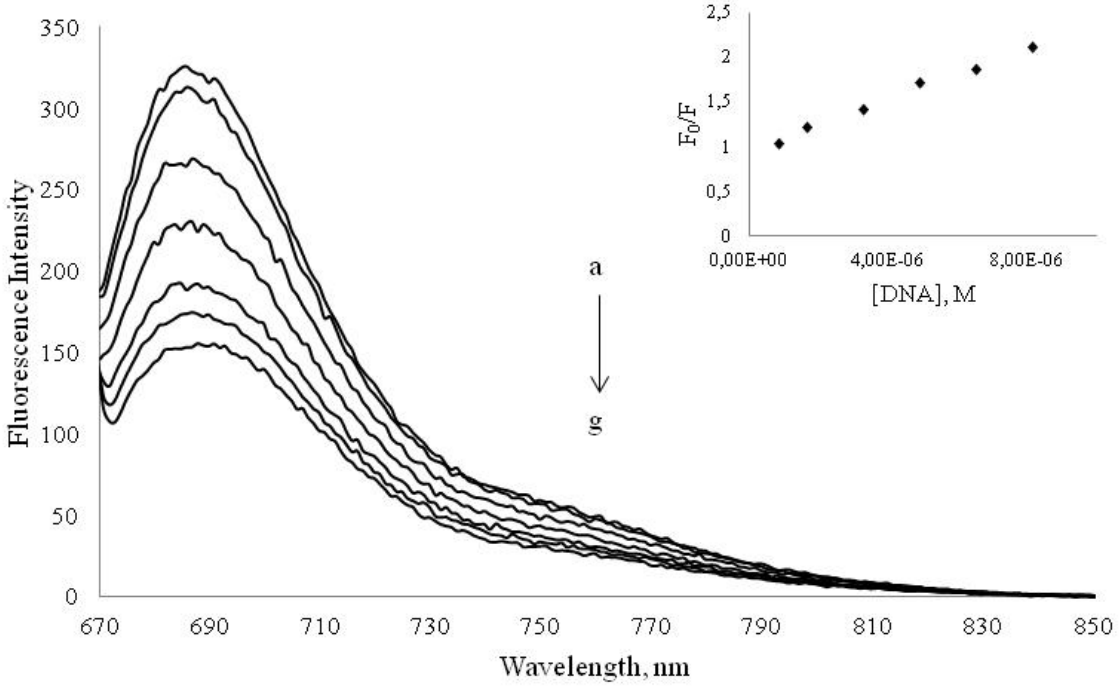

Fig. 6 – Fluorescence spectra of MB in the presence of different concentrations of DNA. C_{MB}= 5.0 ×10^{-6} M (a) and C_{DNA}= 8.13×10^{-7} M (b), 1.62×10^{-6} M (c), 3.25×10^{-6} M (d), 4.87×10^{-6} M (e), 6.5×10^{-6} M (f), and 8.13×10^{-6} M (g). The inset shows Stern-Volmer plot of MB-DNA system.

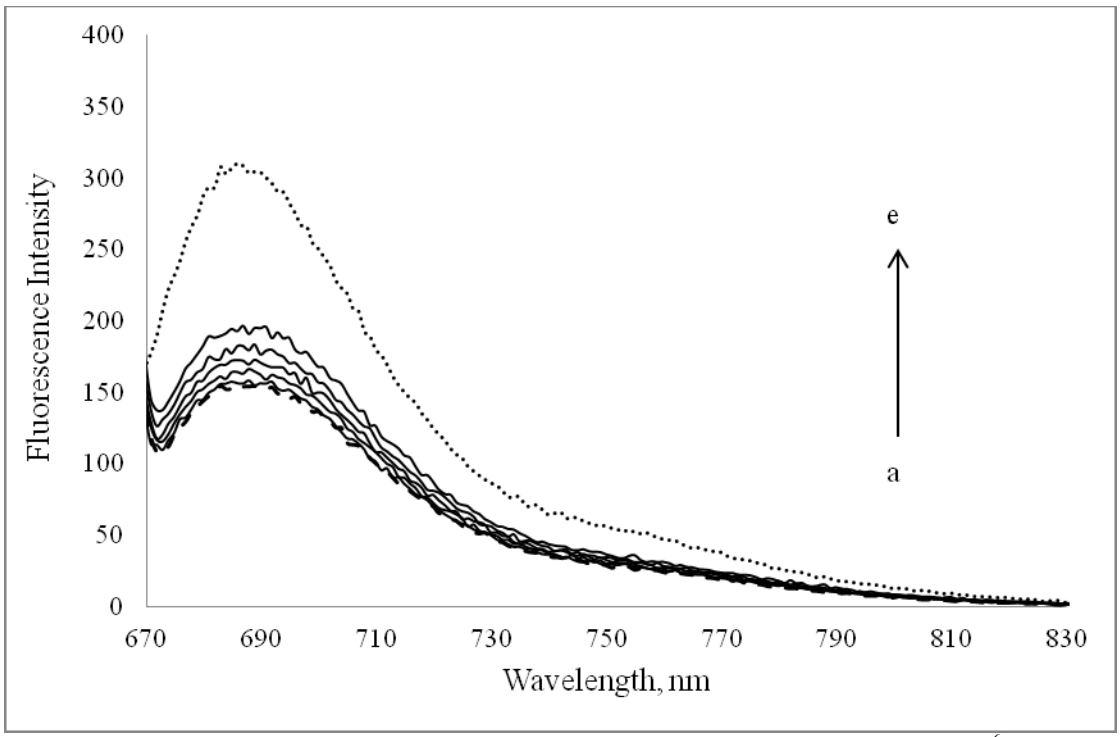

Fig. 7 – Fluorescence spectra of the competitive reaction between TMZ and MB-DNA. C_{MB} = 5.0 ×10^{-6} M (…) and with C_{DNA} = 8.13×10^{-6} M (---) , C_{TMZ} = 2.0×10^{-5} M (a), 4.0×10^{-5} M (b), 6.0×10^{-5} M (c), 8.0×10^{-5} M (d), and 1.0×10^{-4} M (e).

This method is based on the competing binding of MB and TMZ with DNA. Before the TMZ-DNA interaction studies, in the first step, the binding coefficient of MB to DNA was calculated using the UV-vis spectroscopic method. This study was conducted to compare the binding constants of MB

and TMZ with DNA. For this purpose, spectrophotometric titration method was used similarly to TMZ-DNA study. The spectrum of MB showed three main peaks at 247, 293 and 665 nm and shoulders at 329 and 613 nm. With the addition of DNA, decreasing of absorption intensity at 613 nm and red shift were observed. This event shows that MB interacts intercalatively with DNA. From the obtained data, the binding coefficient for MB-DNA was calculated to be 2.2×10^4 M^{-1} using Benesi-Hildebrand equation (Fig. 5).

The quantum yield of DNA and TMZ very low at room temperature and the intrinsic fluorescence of them are not useful practically. Therefore, the use of fluorescence probes needed for identification of DNA-drug interaction. In this study, MB was selected as a probe to investigate the interaction of TMZ with ds-DNA by the spectrofluorimetric method. In the competitive binding experiments, an appropriate quantity of DNA solutions was added step by step to MB solution until the reached stable signal. Fluorescence spectra of the MB in the absence and presence of DNA showed a maximum emission at 686 nm when excitation wavelength was at 665 nm. As shown in Fig. 6, decreased fluorescence intensity of MB at 686 nm was observed in increasing DNA concentration. This quenching effect can be explained by the fact that when a MB interacts with the ds-DNA, photoelectrons would be transferred from the DNA bases to the excited state of the MB which would result in quenching of the fluorescence intensity. This decrease implied that the MB and ds-DNA interaction was intercalation mode. The fluorescence quenching data are analyzed by the Stern–Volmer equation (Eq. (2)).[37]

$$F_0/F = 1 + K_{SV}[Q] \quad (2)$$

where F_0 and F are the fluorescence intensities of MB in the absence and in the presence of ds-DNA, respectively. K_{SV} is the Stern–Volmer quenching constant and [Q] is the concentration of the quencher. K_{SV} was determined by linear regression of a plot of F_0/F against [Q] and found 1.47×10^5 M^{-1} which indicates strong quenching ability of DNA on fluorescence emission of MB (Fig. 6 inset). The quenching of fluorescence is examined in two parts as static and dynamic. In dynamic quenching, quencher and phosphorescent molecule contact when they are at the excited state which causes non-radiative relaxation. However, in static quenching, phosphorescent molecule and the quencher form a non-phosphorescent complex at the ground state. Therefore, absorption spectra of phosphorescent molecule change in static quenching, but no difference is observed in dynamic quenching. In MB-DNA interaction, quenching mechanism is static due to the red shift in absorbance spectra and linearity of Stern-Volmer plot.

For TMZ-DNA interaction studies, the MB-DNA mixture solution giving the lowest signal was prepared freshly and fluorescence measurements were taken after by adding different volumes of TMZ. Upon addition of the TMZ solution onto the MB-DNA complex, the intensity of the fluorescence was recovered due to the released MB molecules because of the formation of the TMZ-DNA complex (Fig. 7). This event has suggested that TMZ may compete with MB to bind DNA through intercalative binding mode at the similar binding site of MB. To determine if this observed effect is due to the TMZ-MB interaction, the TMZ solution was added to the MB solution, but no effect was observed on the emission peak of the MB. This suggests that TMZ does not directly interact with MB, but interacts with MB-DNA complex, resulting in the formation of TMZ-DNA complex.

EXPERIMENTAL

Chemical and Reagents

TMZ and double-stranded DNA (ds-DNA) were purchased Sigma-Aldrich (St. Louis, USA). Chromatographic grade acetonitrile and analytical grade acetic acid, sodium acetate, phosphoric acid, boric acid, HCl, and NaOH were obtained from Merck (Darmstadt, Germany). Double-distilled water with conductivity lower than 0.05 μS/cm was used for the preparation of aqueous solutions.

The preparation of interaction studies solutions

In order to make the preparation of the standard TMZ stock solution, 20.0 mg TMZ was accurately weighed and dissolved in mobile phase in a 100.0 mL volumetric flask and then adjusted to 100.0 mL with the same solution. For the interaction of degradation product and DNA studies, a similar quantity of TMZ was dissolved in 100.0 mL deionized water and then dilutions were done by mobile phase. A ds-DNA solution was prepared by dissolving 40 mg ds-DNA in 100.0 mL deionized water and stored in the refrigerator. After dissolving the fibers in deionized water, the exact concentration of DNA was determined spectrophotometrically from absorbance value at 260 nm (ε_{260} = 6600 L mol^{-1} cm^{-1}). The purity of this solution was checked from the absorbance ratio A_{260} / A_{280}. [34] Commercial ds-DNA samples can be obtained and purified from biological sources such as tissue or cells, therefore, they may have proteins as contaminants. The ratio of absorbance for the ds-DNA solution at 260-280 nm provides an estimate of the purity of DNA with respect to contaminant that absorbs in UV. A value of A_{260} / A_{280} ratio between 1.8 and 1.9 indicates that the protein concentration is

negligible and no further deproteinization is required. The ratio of absorbance from ds-DNA solution was found as 1.86, which indicated that the ds-DNA was free from contamination. Methylene blue (MB) solution used for fluorescence experiments was prepared as $1x10^{-5}$ M in deionized water.

Acetate buffer (0.02 M, pH4.5) was prepared in deionized water and pH was adjusted using sodium hydroxide (5 M). Buffer solution and sodium hydroxide (1 M and 5 M) were prepared using chromatographic grade reagents and deionized water.

For chromatographic experiments, two different solution groups were prepared for the analysis of drug-DNA interaction by HPLC. In the first solution group, 1.0×10^{-5} M DNA concentration was kept constant and TMZ solution was added at 5 different concentrations (5.2×10^{-5} M, 1.3×10^{-4} M, 2.6×10^{-4} M, 3.9×10^{-4} M, 5.2×10^{-4} M). In the second group of solutions, the DNA solution was added at 5 different concentrations (2.03×10^{-6} M, 5.08×10^{-6} M, 1.02×10^{-5} M, 1.52×10^{-5} M, 2.03×10^{-5} M) on the 2.60×10^{-4} M TMZ solution. All the solutions used were prepared in three parallel.

Spectrophotometric titration method was also performed. In the application of this method the assay solutions containing TMZ (8.32×10^{-5} M), various concentrations of DNA (1.66×10^{-6} M, 3.32×10^{-6} M, 4.98×10^{-6} M, 6.64×10^{-6} M, and ve 8.3×10^{-6} M) were prepared in 2.5 mL of acetate buffer. The change of absorbance intensity was recorded.

The quantum yield of DNA is about 10^{-4}-10^{-5} at room temperature; hence, the intrinsic fluorescence of DNA is practical usefulness.[35] In addition to the experimental data, TMZ is also nonfluorescent. The use of fluorescence probes is that they can obtain the information of DNA-drug interaction. In this study, MB was selected as a probe to investigate the interaction of TMZ with ds-DNA by the spectrofluorimetric method. In order to make the application of displacement method, DNA (8.13×10^{-5} M) was added step by step (50-250 μL) to a final concentration of 5.0×10^{-6} M MB solution, until the reached stable signal. After this step, the competitive experiments were conducted by adding small aliquots (50 μL) of TMZ stock solutions (10^{-3} M) to freshly prepared DNA (8.13×10^{-5} M)- MB (5.0×10^{-6} M) complex solution. The change of fluorescence intensity was recorded.

Chromatographic conditions

The HPLC system consisted of a model The Agilent series 1260 solvent delivery system with The Agilent 1260 Diode Array detector system. An ACE C18 column (150×4.6 mm. i.d., 5 μm particle size) was used. The mobile phase used in HPLC was an aqueous acetate buffer (0.02 M)–acetonitrile (90:10, v/v) (pH 4.5). After mixing, mobile phase filtration was performed with Erich Wiegand GmbH type N 022 AN 18 vacuum pump with All tech 47 mm, 0.45 m filter paper. Bondelin Sonorex RK 100 H was used as a degasser. The typical operating conditions were as follows: flow rate, 0.8 mL/min; operating temperature, 30°C; injection volume, 30 μL.

CONCLUSION

In this paper, the interaction of TMZ with DNA in pH 4.5 acetate buffer was investigated by HPLC, UV–vis spectrophotometry, and spectrofluorometry. The interaction of TMZ with DNA resulted in significant changes in chromatographic and spectral characteristics. In chromatographic studies, upon binding to DNA, the peak areas of TMZ and degradation product of TMZ, AIC, showed decreasing and increasing effect, respectively. In addition, obtained data from spectrophotometry has been indicated that TMZ and DNA interacted because of the hypochromic character of TMZ spectra. Due to the non-fluorescence behaviour of TMZ and DNA, MB was used as a fluorescent probe. When TMZ was added to MB-DNA solution, TMZ competed with MB and bound to DNA. Finally, released MB recovered its fluorescence emission. The binding mode of TMZ and ds-DNA will provide necessary information on the mechanism of anticancer drugs' binding with DNA, and they will benefit from the designing of new drugs.

REFERENCES

1. Z. Wang, P. Hu, F. Tang, H. Lian, X. Chen, Y. Zhang, X. He, W. Liu and C. Xie, *Cancer Lett.,* **2013**, *379*, 134-142.
2. S. Lee, *Genes & Diseases,* **2016**, *3*, 198-210.
3. M. F. G. Stevens, J. A. Hickman, S. P. Langdon, D. Chubb, L. Vickers, R. Stone, G. Baig, C. Goddard, N. W. Gibson, J. A. Slack, C. Newton, E. Lunt, C. Fizames and F. Lavelle, *Cancer Res*., **1987**, *47*, 5846-5852.
4. L. L. H. Tsang, C. P. Quarterman, A. Gescher and J. A. Slack, *Cancer Chemother. Pharmacol*., **1991**, *27*, 342-346.
5. J. Wei, R. Zhou, Y. Peng and Y. Liu, *Asian J. Chem*., **2013**, *25*, 2597-2600.
6. J. A. Hartley, N. W. Gibson, K. W. Kohn and W. B. Mattes, *Cancer Res.,* **1986**, *46*, 1943-1947.
7. L. Meer, R. C. Janzer, P. Kleihues and G. F. Kolar, *Biochem. Pharmacol*., **1986**, *35*, 3243-324.
8. A. Khan, S. Imam, M. Aqil, Y. Sultana, A. Ali and K. Khan, *Beni-Suef University J. Basic App. Sci.,* **2016**, *5*, 402-408.
9. E. Gilant, M. Kaza, A. Szlagovska, K. Byczak and P. Rudzki, *Acta Pol. Pharm. Drug Res*., **2012**, *69*, 1347-1355.
10. A. Rao, G. Ramesh and J. Rao, *Asian J. Chem*., **2010**, *22*, 5067-5071.
11. F. Shen, L. A. Decosterd, M. Gander, S. Leyvraz, J. Biollax and F. Lejeune, *J. Chromatogr. B Biomed. Appl.,* **1995**, *19*, 291-300.
12. H. K. Kim, C. C. Lin, D. Parker, J. Veals, J. Lim, P. Likhari, P. Statkevich, A. Marco and A. A. Nomeir, *J. Chromatogr. B Biomed Sci. Appl.,* **1997**, *703*, 225-233.
13. L. Jedynak, M. Puchalska, M. Zezula, M. Laszcz, W. Luniewskib and J. Zagrodzka, *J. Pharm. Biomed. Anal.,* **2013**, *83*, 19– 27.
14. S. Chowdhury, D. Laudicina, N. Blumenkrantz, M. Wirth and K. Alton, *J. Pharm. Biomed. Anal*., **1999**, *19*, 659-668.
15. M. Andrási, B. Törzsök, A. Klekner and A. Gáspár, J. *Chromatogr. B,* **2011**, *879*, 2229–2233.
16. M. H. Khalilian, S. Mirzaei and A. A.Taherpour, *J. Mol. Model,* **2016**, *22*, 270.
17. M. Ghalkhani, I. Fernandes, S. Shahrokhian, S. C. B. Oliveira and A. M. Oliveira-Brett, *Electroanalysis* **2010**, *22*, 2633-2640.

18. I. C. Lopes, S. C. B Oliveira and A. B. Oliveira-Brett, *J. Electroanal. Chem*., **2013**, *704*, 183-189.
19. J. H. Huang, X. M. Wang, D. Fei and L. S. Ding, *App. Spectrosc.,* **2010**, *64*, 1126-1130.
20. S. Agarwal, D. K. Jangir and R. Mehrotra, *J. Photoch. Photobio. B,* **2013**, *120*, 177-182.
21. D. Z. Sun, X. Y. Xu, M. Liu, X. J. Sun, J. Y. Zhang, L. W. Li and Y. Y. Di, *Int. J. Pharm.,* **2010***, 386*, 165-171.
22. C. Ozluer and H. E. Satana Kara, *J. Photoch. Photobio. B.,* **2014**, *138*, 36-42.
23. R. Mehrotra, D. K. Jangir, S. Agarwal, B. Ray, P. Singh and A. K. Srivastava, *MAPAN*., **2013**, *28*, 273-277.
24. C. Cai, X. Chen and F. Ge, *Spectrochim. Acta A*., **2010**, *76*, 202–206.
25. M. L. Yola and N. Ozaltin, *J. Electroanal. Chem.*, **2011**, *653*, 56-60.
26. N. Motohashi, K. Kamata and R. Meyer, *Anticancer Res.,* **1990**, *10*, 1611-1614.
27. A. Karikas, V. Constantinou-Kokotou, V. Magrioti and G. Kokotos, *J. Liq. Chrom. Rel. Technol.,* **2000**, *23*, 1859–1864.
28. A. H. J. Wang, Y. G. Gao, Y. C. Liaw and Y. K. Li, *Biochemistry*, **1991,** *30,* 3812-3815.
29. M. Ryvolova, V. Adam, T. Eckschlager, M. Stiborova and R. Kizek, *Electrophoresis,* **2012**, *33*, 1545–1549.
30. S. N. Topkaya, G. Serindere and M. Ozder, *Electroanalysis,* **2016**, *28*, 1052-1059.
31. C. Altay, E. Eksin, G. Congur and A. Erdem, *Talanta,* **2015**, *144*, 809-815.
32. I. Lopes, S. C. B. Oliveira and A. M. Oliveira-Brett, *Anal. Bianal. Chem., **2013,** 405,* 3783-3790.
33. J. H. Wei, R. H. Zhou, Y. Peng and Y. C. Liu, *Asian J. Chem*., **2013**, *25*, 2597-2600.
34. Y. Lu, G. K. Wang, J. Lv, G. S. Zhang and Q. F. Liu, *J. Fluoresc.,* **2011**, *21*, 409-414.
35. J. P. Morgan and M. Daniels, *Photochem. Photobiol*., **1980**, *31*, 101-113.
36. G. Zhang, A. Wang, T. Jiang and J. Guo, *J. Mol. Struct*., **2008**, *891*, 93-97.
37. J. R. Lakowicz "Principles of Fluorescence Spectroscopy", Second Edition, Plenum Press, New York, 1999.